ISSN: 1231-4005
e-ISSN: 2354-0133
DOI: 10.5604/12314005.1137849

ANALYSIS OF MOTORCYCLIST'S BODY MOVEMENT DURING A MOTORCYCLE IMPACT AGAINST A MOTOR CAR SIDE

Leon Prochowski

Military University of Technology
Gen. S. Kaliskiego Street 2, 00-908 Warsaw, Poland
tel.: +48 22 6837866, fax: +48 22 6837866
e-mail: lprochowski@wat.edu.pl

Tomasz Pusty

Automotive Industry Institute PIMOT
Jagiellońska Street 55, 03-301 Warsaw, Poland
tel.: +48 22 7777084, fax: +48 22 7777020
e-mail: t.pusty@pimot.org.pl

Abstract

The motorcyclist's body motion following a motorcycle impact against a motor car side is determined by a system of forces and reactions acting on the rider's body. An analysis of this motion was carried out, based on a research experiment. The related measurements and calculations were taken as a basis for an analysis of the dynamic loads; they also indicated the type and scope of the bodily injuries that may be incurred by the motorcyclist during a road accident. Based on the research experiment, the trajectory of motorcyclist's head and torso and the course of contact between the motorcyclist's body and the car were determined.

The acceleration values having been obtained from the measurements were used for determining the displacements and changes in the angular position of motorcyclist's head and torso. The research experiment confirmed the motorcyclist's head to be the part of his/her body that undergoes the highest accelerations. The system of forces and reactions acting on motorcyclist's body at the initial stage of the motion under consideration may lead to a situation dangerous to the motorcyclist where his/her head hits the edge of the car roof.

Keywords: *road traffic, road accidents, motorcyclist's safety, motorcyclist's kinematics*

1. Introduction

This study was undertaken to analyse the motorcyclist's body motion during the phase when the motorcycle hits a motor car side. Results of such an analysis will provide a basis for gaining knowledge of the processes of development of the extreme dynamic loads on motorcyclist's head, neck, and torso. This information may be used for improving motorcyclist's safety equipment and elements as well as motorcycle construction. The analysis presented here has been based on the results of measurements carried out at the Automotive Industry Institute (PIMOT) in Warsaw within a research experiment during which a motorcycle with a motorcyclist, moving with a speed of 49.5 km/h, hit a passenger car side (Fig. 1).

The motorcycle hit the front door of the car, close to pillar B. The experiment was prepared in cooperation with the Student Scientific Circle of Vehicle Mechanical Engineers at the Faculty of Automotive and Construction Machinery Engineering of the Warsaw University of Technology; the experiment was organised by Mr J. Seńko, D. Eng. [e-mail: jsenko@simr.pw.edu.pl]. The experiment was carried out in compliance with ISO 13232 standard specifications, with the use of a Ford Sierra car and a Suzuki GS-500 motorcycle. An OPAT OGLE test dummy representing a 50-centile male of 77 kg mass was used as a biomechanical model of the human body. The

motorcyclist dummy was seated on the motorcycle in a position tilted in the direction of ride, corresponding to the typical motorcyclist's posture. The dummy was wearing protective suit, helmet in accordance with requirements of UN ECE Regulation No. 22 "Uniform provisions concerning the approval of protective helmets and their visors for drivers and passengers of motor cycles and mopeds", and leather shoes. Additionally, the dummy had protective gloves on.

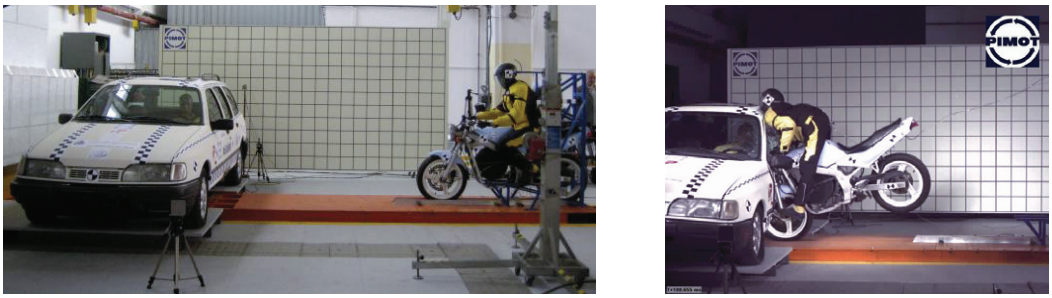

Fig. 1. Positions of the vehicles prior to the collision and at t = 100 ms

The motorcyclist's motion following the motorcycle impact against a car side largely depends on the position in which he/she rode the bike [2, 3]. The motorcyclist's position has an influence on the trajectories of specific parts of his/her body, on the location of the point where the body may hit the car (side window, roof edge, roof panel), and on the bodily injuries he/she might incur in result of the collision.

2. Description of motorcyclist's body motion based on an analysis of the video record

The motorcyclist's body motion following a motorcycle impact against a car side is determined by a system of forces and reactions acting on the rider's body. In the initial phase of the collision, this system of forces consists of the inertia and gravity forces stemming from motorcyclist's mass and of the reaction forces exerted by the motorcycle on the rider's body. The reactions are present in all the areas of contact between the rider and the motorcycle.

The motorcyclist rests on the bike at several places, considered by the authors as single points of contact between these two objects, with an assumption made that these points are situated in the centres of the actual areas of contact. In the initial phase of the collision (until the motorcyclist's helmets hits the edge of the car roof), the force that achieves the highest value is the reaction force exerted by the seat and fuel tank on motorcyclist's hips. The major components of the forces and reactions acting on the motorcyclist at the moment of contact between the motorcycle wheel and the car have been shown in Fig. 2. In result of these forces:

- the rider moves along the motorcycle due to the action of the longitudinal component of the inertia force (F_{CX});
- the forward tilt of motorcyclist's body increases under the influence of, *inter alia*, the moment of the longitudinal component of the inertia force (F_{CX}) and the longitudinal component of the reaction force exerted by the fuel tank on motorcyclist's hips (F_{DX});
- motorcyclist's hips are lifted in relation to the motorcycle in result of the action of the vertical component of the reaction force exerted on them by the fuel tank (F_{DZ}).

The motion of motorcyclist's body was analysed with using a video record of the experiment, taken at a rate of 1 000 fps. Based on this, a contour of the motorcyclist's body in successive positions assumed by the body at 0.01 s time intervals was drawn as presented in Fig. 3. The starting position was defined as the one when the motorcycle wheel came into contact with the car, which corresponded to the instant of 0 ms. Dashed vertical and horizontal lines spaced at 0.5 m intervals have also been plotted in Fig. 3 as a reference dimensional grid.

To facilitate the analysis of the motorcyclist's body motion, four characteristic points were marked on the motorcyclist silhouette. These points represent the markers placed on the helmet

(point A), neck (point B), centre of the torso (point C), and trace of the rotation axis going through the hips (point D). The angle between segments AB and BC defines the bend of the cervical spine. The values of this angle have been specified in Fig. 3. The angle between segment BC and the vertical plane going through point C is the motorcyclist's torso tilt angle.

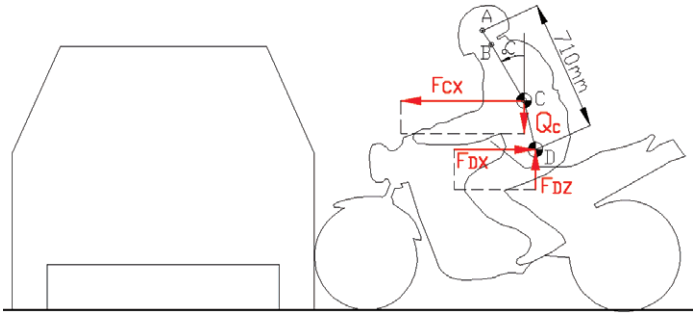

Fig. 2. Forces and reactions acting on the motorcyclist during an impact against a car body: the instant when the motorcycle wheel comes into contact with the car (F_{CX} – longitudinal component of the motorcyclist's inertia force, Q_C – motorcyclist's gravity force, F_{DX} – longitudinal component of the reaction force exerted by the fuel tank on motorcyclist's hips, F_{DZ} – vertical component of the reaction force exerted by the fuel tank on motorcyclist's hips)

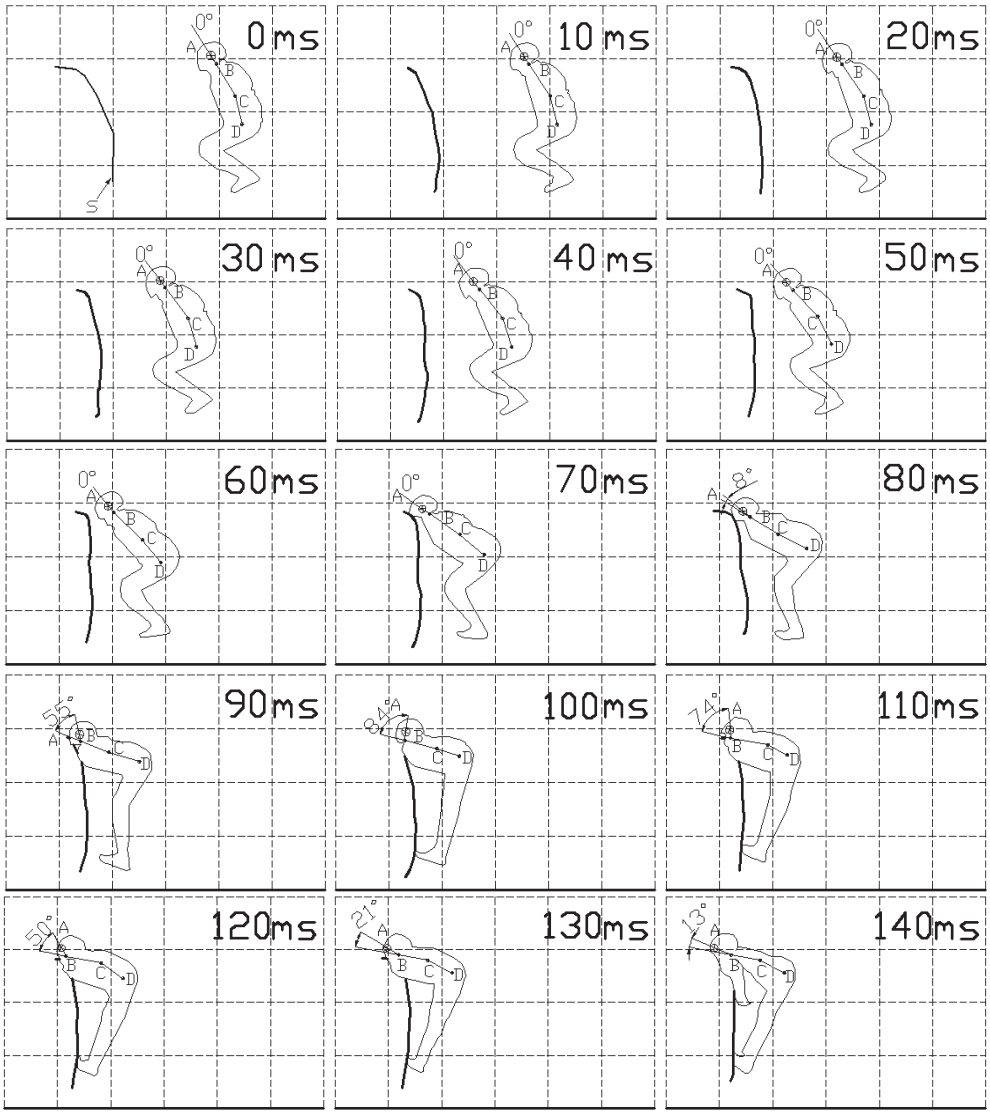

Fig. 3. Positions of the motorcyclist's silhouette at 10 ms time intervals (s – a fragment of the car contour)

The motorcyclist's silhouettes at specific instants, shown in Fig. 3, provide a good basis for an analysis of the motorcyclist's motion following the motorcycle impact against a car side. If the successive positions of points A, B, C, and D are connected in series, the trajectories of the moving motorcyclist's body parts can be drawn.

More details about the motorcyclist's body motion can be found in Fig. 4, where the trajectories of the characteristic points A, B, C, and D (for the successive point positions determined at 20 ms time intervals) have been plotted and a fragment of the car contour, the motorcycle and motorcyclist's position have been drawn for the initial and final time instant.

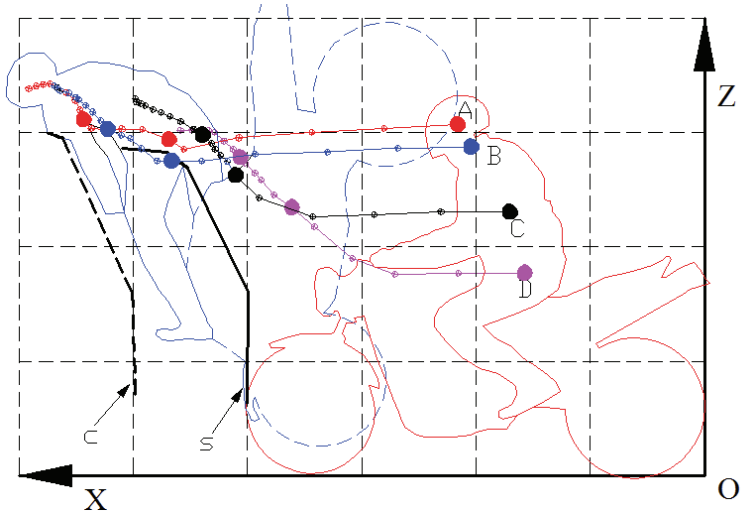

Fig. 4. Motorcycle and motorcyclist's silhouettes with trajectories of points A, B, C, and D (s – a fragment of the car contour at t = 0 ms; c – a fragment of the car contour at t = 380 ms; bold dots show the positions of individual characteristic points at the instants of t = 0 ms, t = 100 ms, and t = 200 ms)

Based on the video record of the experiment and on the motorcyclist's silhouette positions drawn in Fig. 3, and Fig. 4, the major phases of motorcyclist's motion were described, which has been summarized in Tab. 1.

Tab. 1. Major phases of motorcyclist's motion

0 ms	The motorcycle wheel came into contact with the car
about 40 ms	Motorcyclist's hips began to act on the motorcycle fuel tank
about 50 ms	Motorcyclist's hips began to be lifted by the reaction from the fuel tank
75 ms	Motorcyclist's helmet came into contact with the edge of the car roof
90 ms	Motorcyclist's shoulders hit the edge of the car roof
130 ms	Motorcyclist's head moved over the edge of the car roof

From the beginning of the process until the instant of about 50 ms, the motorcyclist moved almost exclusively along the motorcycle, according to the plotted trajectories of points A, B, C, and D. During this movement, friction forces were exerted by motorcyclist's body on the seat and rider's thighs and hips strongly acted on the fuel tank of the motorcycle. After about 50 ms, vertical movement (lifting of motorcyclist's hips) with simultaneous tilting of motorcyclist's body in the direction of motorcycle ride began to be visible in addition to the horizontal motion.

Based on Fig. 4, a graph was prepared (Fig. 5) to show the time histories of changes in the motorcyclist's torso tilt angle, in the distance between points A and D, in the cervical spine bend angle, and in the motorcyclist's head tilt angle (determined by measuring the angular position of marker "A" on dummy's helmet). These curves were then utilized, *inter alia*, to determine the force of impact of motorcyclist's head against the car.

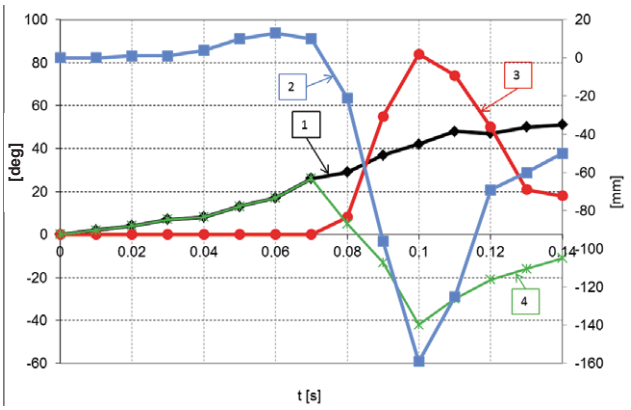

Fig. 5. Time histories of changes in the motorcyclist's torso tilt angle (1), in the distance between points A and D (2), in the cervical spine bend angle (3), and in the motorcyclist's head tilt angle (4)

During the experiment carried out, the motorcyclist's torso tilt angle (α, see Fig. 2) changed from 30° at $t = 0$ ms to 60° at $t = 80$ ms, i.e. immediately after the impact of motorcyclist's helmet against the car. The tilt of motorcyclist's torso affects the location of the point of impact of motorcyclist's head against the car (e.g. the edge of the car roof). The impact of motorcyclist's head against the edge of the car roof was followed by bending the head backwards, which resulted in a change in the value of the cervical spine bend angle and in the distance between points A and D (compression, see Fig. 4 and 5).

3. Analysis of motorcyclist's body motion based on dynamic measurements

The values of the accelerations to which the human body is exposed during a road accident usually provide grounds for an analysis of the related dynamic loads and indicate the cause, type, and scope of the injuries incurred. The acceleration sensors placed in motorcyclist's head and torso as shown in Fig. 6 and Fig. 7 recorded the acceleration components in the three mutually perpendicular directions a_{Gx}, a_{Gy}, and a_{Gz} (in dummy's head) and a_{Tx}, a_{Ty}, and a_{Tz} (in dummy's torso). The lateral acceleration components a_{Gy}, and a_{Ty} were not analysed because of negligible lateral motions of the motorcyclist.

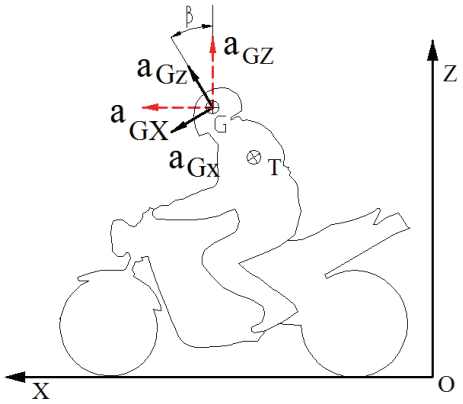

Fig. 6. Position of the measurement axes of the sensors of accelerations a_{Gx} and a_{Gz} in dummy's head and directions of the calculated components of the acceleration vector

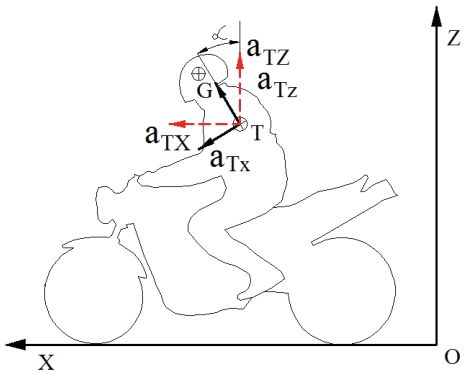

Fig. 7. Position of the measurement axes of the sensors of accelerations a_{Tx} and a_{Tz} in dummy's torso and directions of the calculated components of the acceleration vector

The measured time histories of motorcyclist's head and torso acceleration components (a_{Gx} and a_{Gz} for the head and a_{Tx} and a_{Tz} for the torso) were used for determining the acceleration components in the global reference frame (with axes OX and OZ), i.e. a_{GX} and a_{GZ} for the head

and a_{TX} and a_{TZ} for the torso. The components a_{GX}, a_{GZ}, a_{TX}, and a_{TZ} in the global reference frame were calculated with taking into account the previously determined time histories of changes in the values of angles α and β, i.e. the angles of tilt of motorcyclist's torso and head together with corresponding acceleration sensors, respectively (see Fig. 6 and Fig. 7), i.e. according to the following formulas:

$$a_{GX}(t) = a_{Gx}(t)\cos\beta(t) + a_{Gz}(t)\sin\beta(t), \tag{1}$$

$$a_{GZ}(t) = -a_{Gx}(t)\sin\beta(t) + a_{Gz}(t)\cos\beta(t), \tag{2}$$

$$a_{TX}(t) = a_{Tx}(t)\cos\alpha(t) + a_{Tz}(t)\sin\alpha(t), \tag{3}$$

$$a_{TZ}(t) = -a_{Tx}(t)\sin\alpha(t) + a_{Tz}(t)\cos\alpha(t), \tag{4}$$

where:
a_{GX}, a_{GZ} – motorcyclist's head acceleration components;
a_{TX}, a_{TZ} – motorcyclist's torso acceleration components;
α – motorcyclist's torso tilt angle (curve 1 in Fig. 5);
β – motorcyclist's head tilt angle (curve 4 in Fig. 5).

Results of calculations of the a_{GX}, a_{GZ}, a_{TX}, and a_{TZ} values have been presented in Fig. 8 and 9, where the values of displacements of motorcyclist's head (x_G, z_G) and torso (x_T, z_T) along axes OX and OZ, respectively, have also been shown.

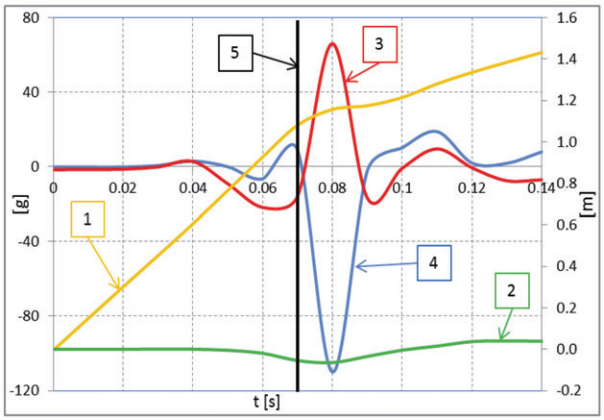

Fig. 8. Summary of changes in motorcyclist's head accelerations and displacements: 1 – x_G, 2 – z_G, 3 – a_{GZ}, 4 – a_{GX}, 5 – the instant when motorcyclist's helmet hit the edge of the car roof

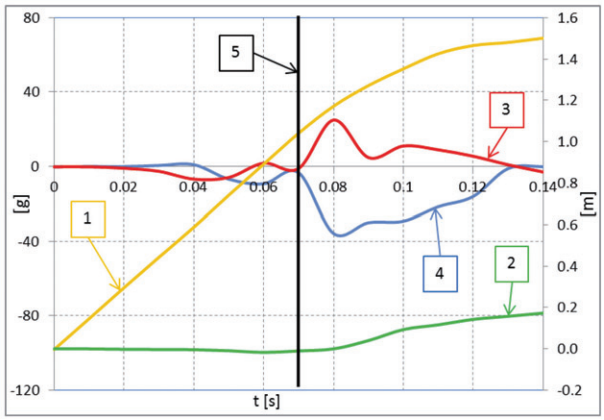

Fig. 9. Summary of changes in motorcyclist's torso accelerations and displacements: 1 – x_T, 2 – z_T, 3 – a_{TZ}, 4 – a_{TX}, 5 – the instant when motorcyclist's helmet hit the edge of the car roof

The rapid growth in the head accelerations, visible in Fig. 8 at the instant of $t = 74$ ms, indicates the beginning of contact of motorcyclist's helmet with the edge of the car roof. Until that time, motorcyclist's head moved by about 1.1 m in the horizontal direction (in accordance with motorcyclist's displacement) and by about 0.1 m in the vertical direction (downwards).

The research experiment confirmed the motorcyclist's head to be the part of his/her body that undergoes the highest accelerations. The head acceleration components along axes OX and OZ at the instant when motorcyclist's helmet hit the edge of the car roof reached values of $a_{GX} = 110$ g and $a_{GZ} = 66$ g, respectively.

Based on the time histories of the head and torso acceleration components (a_{GX} and a_{GZ} as well as a_{TX} and a_{TZ}, respectively), the values of the corresponding head and torso velocity components (v_{GX} and v_{GZ} as well as v_{TX} and v_{TZ}, respectively) were calculated by numerical integration. The calculation results can be seen in Fig. 10 and 11, where the velocity of the motorcycle centre of mass has also been presented for comparison in the form of velocity vs. time curves plotted as appropriate for the velocity components along axes OX and OZ, i.e. v_{CX} and v_{CZ}.

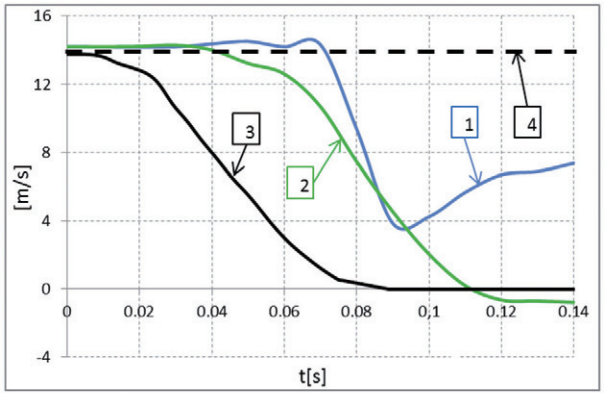

Fig. 10. Time histories of changes in the longitudinal components of the velocities of: motorcyclist's head (v_{GX}, curve 1) and torso (v_{TX}, curve 2) and motorcycle centre of gravity (v_{CX}, curve 3), 4 – initial velocity of the motorcycle impact against the car

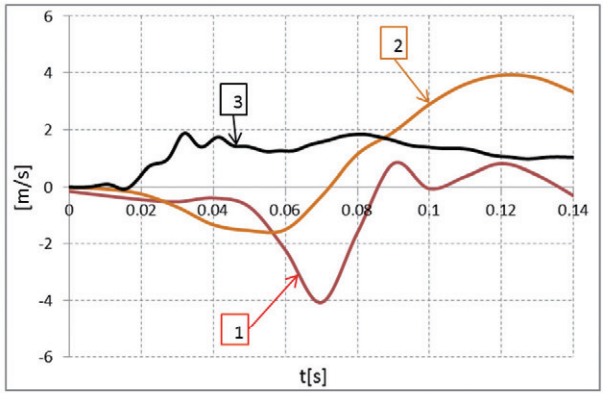

Fig. 11. Time histories of changes in the vertical components of the velocities of: motorcyclist's head (v_{GZ}, curve 1) and torso (v_{TZ}, curve 2) and motorcycle centre of gravity (v_{CZ}, curve 3)

At the instant of about 40 ms, motorcyclist's hips began to act on the motorcycle fuel tank. This interaction resulted in a reduction in the velocity of motion of motorcyclist's torso (visible in Fig. 10) and in tilting of motorcyclist's body in the direction of motorcycle ride (curve 1 in Fig. 5). The tilting of motorcyclist's body in the direction of motorcycle ride led to an impact of rider's head together with the helmet against the edge of the car roof. The head impact velocity components along axes OX and OZ were 14.2 m/s and 4 m/s, respectively (Fig. 10 and 11).

Based on the time histories of the head and torso acceleration components (a_{GX} and a_{GZ} as well as a_{TX} and a_{TZ}, respectively), the values of components of the force of impact of motorcyclist's head against the edge of the car roof were calculated in accordance with the sketch shown in Fig. 12.

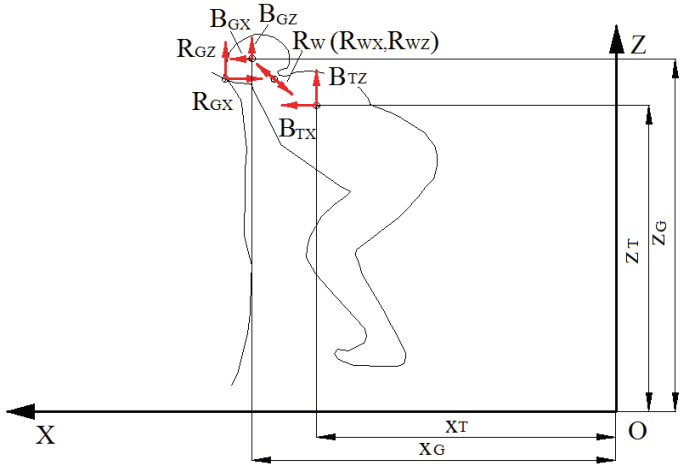

Fig. 12. Sketch utilized to calculate the force of impact of motorcyclist's head against the edge of the car roof

Based on the sketch shown in Fig. 12, the following equations were derived to make the calculations:

$$R_{GX} = B_{GX} + R_{WX} = B_{GX} + B_{TX}\,, \tag{5}$$

$$R_{GZ} = -B_{GZ} - R_{WZ} = -B_{GZ} - B_{TZ}\,. \tag{6}$$

The motorcyclist's head with the helmet was found to have struck the edge of the car roof with a force of R_{GX} = 23 kN, R_{GZ} = 16 kN.

These values were obtained at the head impact velocity components determined as $v_{GX} = 14.2$ m/s and $v_{GZ} = 4$ m/s (see Fig. 10 and 11). At the works reported in [11, 12], the force values determined at head impact velocities of 7.5–10 m/s ranged from 15 to 45 kN.

4. Determining the uncertainty of calculations of the acceleration of motorcyclist's head

The calculation results obtained by analysing the video record and direct measurements are burdened with an uncertainty interval. Therefore, as an example, the values of motorcyclist's head accelerations along axes OX and OZ depended on the values of the following variables (cf. (1)-(4)):

$$a_n = f(a_{Gx}, a_{Gz}, \beta),$$

where a_n defines the values of motorcyclist's head accelerations along axes OX and OZ.

The total uncertainty of the values of motorcyclist's head accelerations along axis OX was calculated with making use of the following formula [10]:

$$\Delta a_{GX}(t) = \left|\frac{\partial a_{GX}(t)}{\partial a_{Gx}(t)}\right| \Delta a_{Gx}(t) + \left|\frac{\partial a_{GX}(t)}{\partial a_{Gz}(t)}\right| \Delta a_{Gz}(t) + \left|\frac{\partial a_{GX}(t)}{\partial \beta(t)}\right| \Delta\beta \,. \tag{7}$$

The uncertainty of the acceleration values recorded was assumed as 2% of the measured value, according to the accuracy of the whole measuring path, i.e. $\Delta a_{Gx} = 2\% a_{Gx}$, $\Delta a_{Gz} = 2\% a_{Gz}$. The uncertainty of measurements of angle β was dictated by the method used to read data from the video record of the experiment; it is equal to $\Delta\beta = 1° = 0.014$ rad. The calculated uncertainty of the motorcyclist's head acceleration values have been given as an example in Tab. 2.

Tab. 2. Results of calculations of the uncertainty of motorcyclist's head acceleration values

Time [s]	a_{GX} [g]	a_{GZ} [g]	Δa_{GX} [g]	Δa_{GZ} [g]
0.04	3.0	2.8	0.1	0.1
0.06	-6.5	-21.9	0.6	0.6
0.08	-110	66	3.26	3.24

The calculated uncertainty of the motorcyclist's head acceleration values is within the range from 1% to 9%, i.e. it has an insignificant impact on the calculations of the force of impact of motorcyclist's head against the edge of the car roof.

5. Summary

The analysis of motorcyclist's body motion, based on a research experiment and on measurement and calculation results, made it possible to determine the trajectories of motorcyclist's head and torso as well as time histories of changes in the head and torso tilt angles and in the cervical spine bend angle. The calculations to be carried out had to be indispensably preceded by a frame-by-frame analysis of the video record of the experiment, aimed at determining the instantaneous values of the angles of tilt of the head and torso together with the sensors installed in them. This analysis revealed that from the beginning of the process till the instant of about 50 ms, the motorcyclist moved almost exclusively along the motorcycle. During this phase of motorcyclist's body motion, firm pressure was applied by rider's thighs and hips on the fuel tank of the motorcycle. The accompanying reaction from the motorcycle caused the motorcyclist's torso to tilt at an increasing angle in the direction of motorcycle ride. The tilting process led to a situation dangerous to the motorcyclist where his/her head hit the edge of the car roof.

The results of measurements of the head and torso acceleration components were utilized for determining the acceleration, velocity, and displacement components in the global reference frame,

thanks to which the velocity and force of impact of motorcyclist's head against the edge of the car roof was calculated. In terms of the vector components along axis OX, the head hit the car with a velocity of 14.2 m/s and a force of 23 kN and the maximum acceleration value measured in the centre of mass of the head reached a level of 110 g. This information is important for the engineering of motorcyclist's safety equipment, including the motorcycle helmet.

References

[1] Grandel, J., Schaper, D., Berg, F. A., *Aufprallmechanik, Kopfbelastung und Schutzhelmwirkung bei Motorrad/Personenwagen-Kollisionen*, ATZ, Nr. 3, 1985.

[2] Grandel, J., Schaper, D., Berg, F. A., *Untersuchung der Motorrad-, Fahrer- und Beifahrer-sicherheit bei Motorradunfallen mit zwei Motorradaufsassen – Teil 1*, ATZ, Nr. 89 (11), 1987.

[3] Grandel, J., Schaper, D., Berg, F. A., *Untersuchung der Motorrad-, Fahrer- und Beifahrer-sicherheit bei Motorradunfallen mit zwei Motorradaufsassen – Teil 1*, ATZ, Nr. 89 (12), 1987.

[4] Prochowski, L., Pusty, T., *Charakterystyka obrotu i unoszenia motocykla po uderzeniu w bok samochodu (Analysis of the rotation and lifting of a motorcycle following an impact against a motor car side)*, The Archives of Automotive Engineering – Archiwum Motoryzacji, Nr 4, 2012,

[5] UN ECE Regulation No. 22. *Uniform Provisions Concerning the Approval of Protective Helmets and Their Visors for Drivers and Passengers of Motor Cycles and Mopeds*.

[6] Prochowski, L., Unarski, J., Wach, W., Wicher, J., *Podstawy rekonstrukcji wypadków drogowych (Fundamentals of the reconstruction of road accidents)*, WKiŁ, Warszawa 2008.

[7] Newman, J., Barr, C., Beusenberg, M., Fournier, E., Shewchenko, N., Welbourne, E., Withnall, C., *A New Biomechanical Assessment of Mild Traumatic Brain Injury. Part 2 – Results and Conclusions*, International Research Council on the Biomechanics of Injury (IRCOBI), Montpelier 2000.

[8] Rücker, P., Berg, F. A., *Der Motorradairbag – neueste Ergebnisse aus Full-Scale-Tests nach ISO 13232*, VKU Verkehrsunfall und Fahrzeugtechnik, Ausgabe Nr. 5, 2005.

[9] Murri, R., *Sicherheitsgurt für Motorräder – Lösungsansätze, Schutzpotenzial und Crashergebnisse*, Verkehrsunfall und Fahrzeugtechnik, Nr. 45, 2007.

[10] Szydłowski, H., *Teoria pomiarów (The Theory of Measurements)*, Państwowe Wydawnictwa Naukowe, Warszawa 1981.

[11] Pinnoji, K. P., Haider, Z., Mahajan, P., *Design of Motorcycle Helmets: Computational Fluid and Impact Analysis*, International Journal of Crashworthiness, Vol. 13, No. 3, pp. 265-278, 2008.

[12] Pinnoji, P. K., Bourdet, N., Mahajan, P., Willinger, R., *New Motorcycle Helmets with Metal Foam Shell*, 2008 IRCOBI Conference Proceedings, Bern, Switzerland 2008.

[13] Prochowski, L., Żuchowski, A., *Comparative Analysis of Frontal Zone of Deformation in Vehicles with Self-Supporting and Framed Bodies*, Journal of KONES Powertrain and Transport, Vol. 18, No. 4, pp. 397-404, 2011.